ADVANCING EARTH AND SPACE SCIENCES

Geophysical Research Letters

RESEARCH LETTER
10.1029/2026GL122536

Zinc Isotopes Reveal Cross-Border Transport of Coal Combustion Pollutants Across the Himalayas During the Summer Monsoon

Xiaoyu Jiao[1], Zhiwen Dong[1], Yaping Shao[2], Giovanni Baccolo[3], Fangzhou Li[4], and Rui Wu[5]

[1]Hubei Key Laboratory of Regional Ecology and Environmental Change, School of Geography and Information Engineering, China University of Geosciences, Wuhan, China, [2]Institute for Geophysics and Meteorology, University of Cologne, Cologne, Germany, [3]Department of Sciences, University of Roma Tre, Rome, Italy, [4]Laboratory for Climate and Environmental Sciences, CEA-CNRS-UVSQ, University Paris-Saclay, Gif-sur-Yvette, France, [5]Northwest Institute of Eco-Environment and Resources, Chinese Academy of Sciences, Lanzhou, China

Key Points:

- Zn isotopes show South Asian coal emissions cross the Himalayas and reach the Tibetan Plateau
- Low elevations reflect smelting source, while high elevations are dominated by coal combustion inputs
- Topography-driven circulation enables long-range transport of anthropogenic metals across the divide

Supporting Information:

Supporting Information may be found in the online version of this article.

Correspondence to:

Z. Dong,
dongzhiwen@cug.edu.cn

Citation:

Jiao, X., Dong, Z., Shao, Y., Baccolo, G., Li, F., & Wu, R. (2026). Zinc isotopes reveal cross-border transport of coal combustion pollutants across the Himalayas during the summer monsoon. *Geophysical Research Letters*, *53*, e2026GL122536. https://doi.org/10.1029/2026GL122536

Received 19 FEB 2026
Accepted 12 JUN 2026

Author Contributions:

Conceptualization: Yaping Shao
Investigation: Xiaoyu Jiao, Zhiwen Dong, Rui Wu
Methodology: Giovanni Baccolo, Fangzhou Li
Software: Fangzhou Li
Supervision: Zhiwen Dong
Writing – original draft: Xiaoyu Jiao
Writing – review & editing: Xiaoyu Jiao, Zhiwen Dong, Yaping Shao, Giovanni Baccolo

Abstract The Himalayas form a major atmospheric barrier between South Asia and Tibetan Plateau, yet cross-barrier transport of anthropogenic metals remains poorly constrained. We use moss δ^{66}Zn along a 750–4,100 m a.s.l. south-north transect in Motuo to trace pollution sources and transport processes. On the southern slope, trace metals (Zn, Pb, As, Ni, Co) display pronounced altitudinal gradients, with low elevations showing high concentrations and light δ^{66}Zn (−0.41‰ to −0.32‰) dominated by smelting (42%–50%). With increasing elevation, concentrations decrease and δ^{66}Zn becomes heavier (0.20‰ to 0.29‰), reflecting greater coal combustion inputs (35%–50%). North of the crest, overall metal loads are lower, but high elevations (>3,500 m) show heavy δ^{66}Zn (0.30‰ to 0.44‰) and strong coal contributions (43%–54%). Our results show that topography, anthropogenic emissions, and vegetation coverage regulate vertical pollutant distribution patterns, providing direct Zn isotopic evidence for transboundary transport of coal combustion emissions from South Asia to the Tibetan Plateau.

Plain Language Summary The Himalayas act as a natural barrier between South Asia and the Tibetan Plateau, but it is not clear how human-made heavy metals can cross this barrier. Here we used stable zinc isotopes (δ^{66}Zn) to track pollution sources and pathways along a south-north mountain transect (750–4,100 m a.s.l.). On the southern slope, metals such as Zn, Pb, As, Ni, and Co show clear patterns with elevation. At low elevations, metal concentrations are high and δ^{66}Zn values are low (−0.41‰ to −0.32‰), mainly due to nearby industrial emissions, especially factory smelting (42%–50%). As elevation increases, metal levels decrease and δ^{66}Zn becomes higher and more stable (0.20‰ to 0.29‰), showing a growing contribution from fine particles transported over long distances from coal burning (35%–50%). On the northern slope, metal levels are generally lower, but at high elevations (>3,500 m a.s.l.), metals become enriched again, with high δ^{66}Zn values (0.30‰ to 0.44‰) and a strong influence from coal combustion (43%–54%). Overall, the topography, human emissions, and vegetation cover together control the vertical distribution of metal concentrations. Emissions from South Asian coal combustion can cross the Himalayas and affect the atmospheric environment of the inner Tibetan Plateau.

1. Introduction

With accelerating industrialization, heavy metals such as Zn, As, Pb, Ni, and Co are increasingly released into the atmosphere through industrial activities, transportation, and energy production, posing a growing global environmental concern (Sen & Peucker-Ehrenbrink, 2012; Tian et al., 2015; Zhu et al., 2020). These elements are toxic, bioaccumulative, and capable of long-range atmospheric transport, reaching remote regions including polar areas and the Tibetan Plateau (Elsen et al., 2020; He et al., 2023; H. Zhang et al., 2013). In mountainous environments, complex terrain and strong elevation gradients modify airflow and enhance deposition, often concentrating pollutants on windward slopes and within valley systems (Bing et al., 2019). Altitudinal variations in climate and vegetation further regulate scavenging efficiency and surface retention, producing pronounced spatial heterogeneity and complicating the identification of transport pathways across major mountain barriers (Bing et al., 2018; T. Li et al., 2017; Musah et al., 2025; Wu et al., 2014). As the “Third Pole,” the Tibetan Plateau plays a key role in the Earth system by influencing the Asian monsoon, regional hydrology, and large-scale atmospheric circulation (Yao et al., 2022).

Stable zinc isotopes (δ^{66}Zn) provide source-specific information linked to emission processes and have become an effective tracer for atmospheric source apportionment (Duan et al., 2025; Schleicher & Weiss, 2023; Schleicher et al., 2020). Different anthropogenic activities generate distinct isotopic signatures. Coal combustion typically produces positive δ^{66}Zn values (+0.17‰ to +1.66‰) through evaporation–condensation fractionation, whereas high-temperature metal smelting preferentially emits isotopically light Zn, resulting in negative values (−0.21‰ to −0.09‰) (Gelly et al., 2019; Mattielli et al., 2009; Ochoa Gonzalez & Weiss, 2015; Wei et al., 2025). Non-exhaust traffic sources, such as brake and tire wear (−0.03‰ to +0.58‰), and re-suspended road dust (−0.03‰ to +0.34‰), also show characteristic isotopic compositions distinct from combustion-related emissions (Borrok et al., 2010; Jeong et al., 2022; Wu et al., 2024). These differences allow δ^{66}Zn to be used to quantify source contributions and trace atmospheric transport processes (Bunnell et al., 2025; S. Dong et al., 2013; Kim et al., 2025).

Although the Tibetan Plateau is relatively pristine, the adjacent South Asia region represents one of the world's major pollution hotspots (Z. Dong et al., 2020; Reddington et al., 2019; Xu et al., 2023). Rapid growth in fossil fuel consumption and industrial output has created high-intensity emissions. By 2012 India consumed approximately 0.68 billion tons of coal and produced approximately 3.6 million tons of non-ferrous metals (Zhu et al., 2020). Coal combustion contributes substantially to Pb, Cr, Mn, and Zn emissions (35%–97%) and dominates As (~60%) and Cr (~96%) emissions, whereas metal smelting contributes 51%–77% of As, Cd, and Ni emissions (Yu et al., 2022; Zhu et al., 2020). The Himalayas act both as a topographic barrier and a dynamic modifier of atmospheric flow, producing strong contrasts in pollutant deposition between southern and northern slopes (Dhungel et al., 2018; M. Zhang et al., 2020; Y. Zhang et al., 2020). Despite increasing evidence for such trans-Himalayan transport, the vertical distribution of pollutants and the relative importance of different sources in high-mountain environments remain poorly constrained (Bing et al., 2018; Hong et al., 2009; Nizam et al., 2020).

Mosses provide an effective biomonitoring medium because they accumulate atmospheric inputs directly, exhibit minimal isotopic fractionation, and lack root uptake. Their high surface area and physiological sensitivity allow them to record both elemental concentrations and isotopic signatures of atmospheric deposition (Cloquet et al., 2008; Dolgopolova et al., 2006). In this study, moss samples were collected along a 750–4,100 m elevational transect across the southern and northern slopes of the Himalayas in the Motuo region. Concentrations of five atmospheric-related metals (Zn, Pb, As, Ni, and Co) and Zn isotopic composition (δ^{66}Zn) were measured to characterize vertical distribution patterns and their controlling factors. Zinc isotopic fingerprints were further used in a mixing framework to quantify anthropogenic and natural source contributions. The results provide new constraints on trans-Himalayan pollutant transport and its implications for atmospheric contamination of the Tibetan Plateau interior.

2. Methodology

2.1. Site Description and Sampling

This study focuses on the Yarlung Tsangpo Grand Canyon in eastern Himalaya (Figure 1a), where vertical transects on both the southern and northern slopes of the canyon were selected for moss sampling. Located on the southern edge of the Tibetan Plateau, the region features a complex geography and diverse climates, representing a pronounced climatic transition zone. Tropical and subtropical monsoon climates dominate the low-elevation valleys near Motuo county, while climate conditions shift progressively to cold temperate and alpine climates with increasing elevation toward the plateau interior. This strong altitudinal climatic gradient makes the region highly sensitive to atmospheric transport and orographic precipitation processes (H. Li et al., 2016). It is both a key site for climate change research and an important corridor for transboundary transport of heavy metal pollutants across the Himalayas (Cai et al., 2024; Yan et al., 2020) (Figure 1).

Sample data are summarized in Table S1 in Supporting Information S1. On the southern slope, 17 moss samples (*Bryum*) were collected along altitudes ranging from 750 to 3,950 m a.s.l., with sampling points set at 200 m elevation intervals to capture vertical variations in heavy metal deposition (red symbols in Figure 1b). The southern slope exhibits typical windward characteristics, with a humid climate and abundant precipitation, exceeding 2000 mm annually in low-altitude areas. For comparison, 8 moss samples (*Bryum*) were collected on the northern slope between 2,700 and 4,100 m a.s.l., also at 200 m intervals (orange symbols in Figure 1b). Situated in the Himalayan rain shadow, the northern slope experiences drier conditions, with precipitation

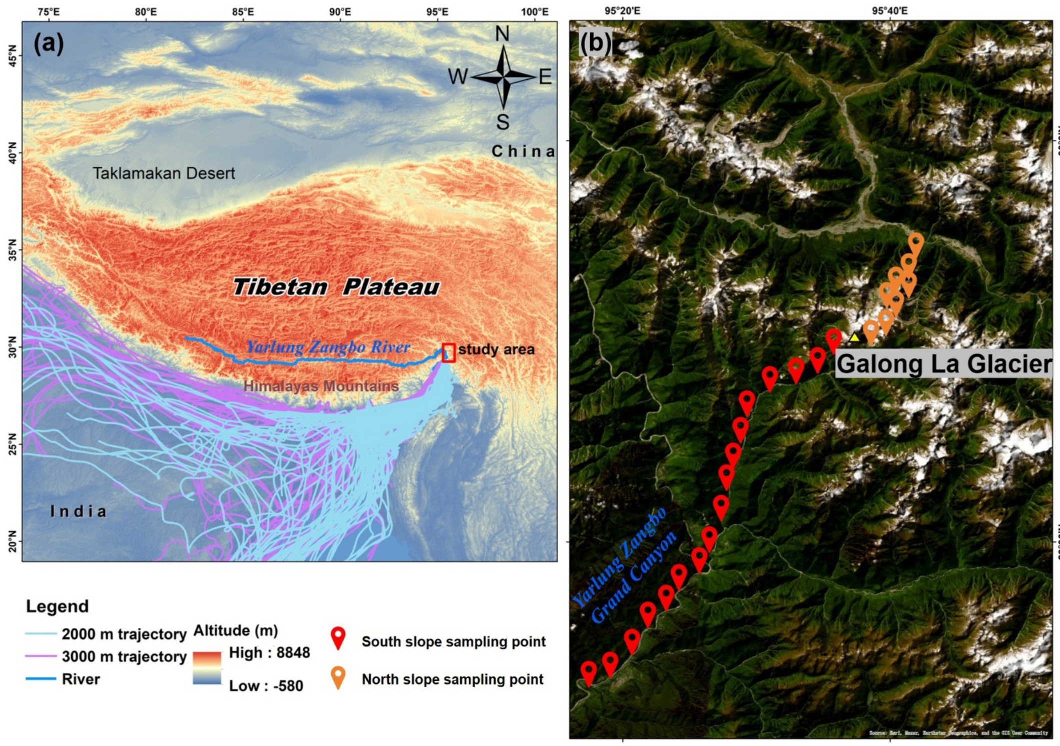

Figure 1. Study area and sampling locations on the Tibetan Plateau. (a) Geographic location of the study region and the 120-hr backward air mass trajectory in the study area during the sampling. (b) Sampling sites, with red symbols indicating sites on southern slopes and orange symbols indicating sites on northern slopes.

concentrated in the summer monsoon season and sparse vegetation dominated by alpine meadows and shrublands (M. Zhang et al., 2020; Y. Zhang et al., 2020).

2.2. Isotope and Element Concentration Measurements

Moss samples were rinsed with ultrapure water to remove surface contaminants and dried at 40°C. Dried materials were homogenized by grinding to fine powders and stored in polyethylene bags. Grinding tools were cleaned with ethanol between samples. Subsequently, samples were digested in Teflon beakers using a mixture of 2.5 mL HNO_3 and 0.5 mL H_2O_2 on a hot plate at 200°C and evaporated to near dryness. After cooling, the residues were dissolved in 0.5 mL HCl and diluted to 25 mL with double distilled deionized water (Bing et al., 2018). Concentrations of Zn, Co, Ni, Pb, As, and Al were measured by ICP-MS (Element XR, Thermo Fisher Scientific, USA), calibrated against SPEX™ standard solutions. Analytical accuracy and precision were evaluated using procedural blanks, duplicate samples, and certified reference materials (GBW07603 and GBW07604). Recoveries exceeded 98%, and analytical precision was better than ±5% RSD.

Prior to isotope analysis, zinc was purified from pretreated samples using an anion-exchange chromatography method. The samples were loaded onto columns packed with pre-cleaned resin (AG MP-1M, 100–200 mesh, Bio-Rad, USA). Columns were sequentially rinsed with ~8 M HCl +0.01‰ H_2O_2 and ~2 M HCl +0.01‰ H_2O_2 to remove matrix elements. After discarding ~2 mL of 0.5 M HNO_3, zinc was eluted in the subsequent ~10 mL of 0.5 M HNO_3. The collected fractions were evaporated to dryness at 80°C and redissolved in ~1 mL of 3% HNO_3 for isotopic measurement. Zinc isotopes were measured using a multi-collector inductively coupled plasma mass spectrometer (MC-ICP-MS, Neptune Plus). The accuracy and precision of the measurements were evaluated through long-term analyses of the geological standard reference material BCR-2. Zinc isotope compositions in this study are reported in δ notation relative to the IRMM-3702 standard, a pure synthetic zinc provided by the Institute for Reference Materials and Measurements, based on the $^{66}Zn/^{64}Zn$ ratio: $\delta^{66}Zn = [(^{66}Zn/^{64}Zn)_{sample}/(^{66}Zn/^{64}Zn)_{IRMM} - 1] \times 1{,}000$.

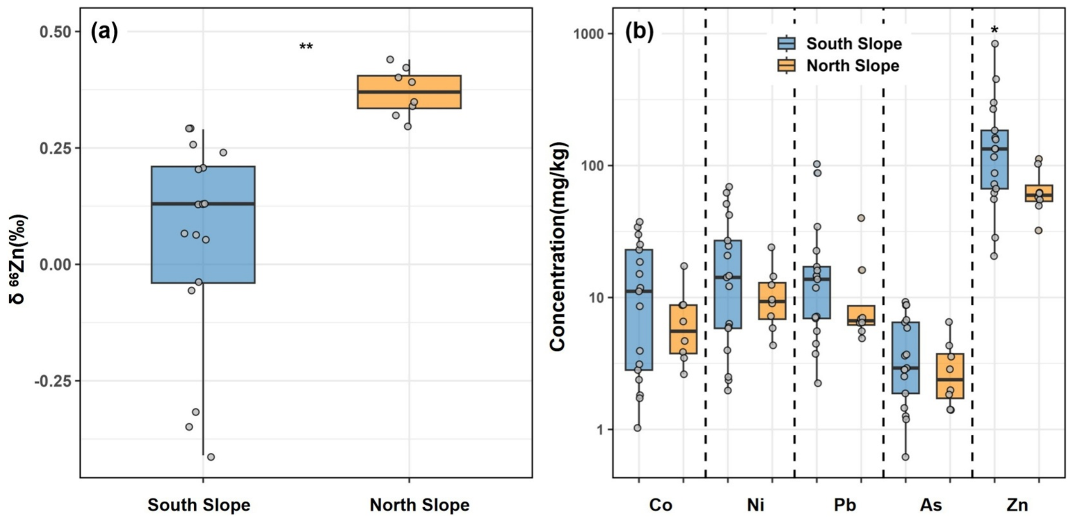

Figure 2. Comparisons of (a) δ^{66}Zn values and (b) metal concentration between the south and north slopes. Boxplots show the median (center line), interquartile range (IQR; box), and 1.5 × IQR whiskers. Shaded boxes in blue and orange correspond to the south and north slopes, respectively. Significance between slopes was evaluated using two-sample Welch's *t*-tests, with $p < 0.05$ (*) and $p < 0.01$ (**).

3. Results

3.1. Zn Isotopic Compositions and Metal Concentrations Across the South and North Slopes

Zinc isotopic compositions differed significantly between the southern and northern slopes (Welch's *t*-test, $p < 0.01$), with lower δ^{66}Zn values on the southern slope (Figure 2a). The southern slope exhibited a broad isotopic range (−0.41‰ to 0.29‰; mean = 0.05 ± 0.44‰, 2σ, $n = 17$), whereas the northern slope a narrower and consistently heavier δ^{66}Zn distribution (0.30‰ to 0.44‰; mean = 0.37 ± 0.10‰, 2σ, $n = 8$).

Zinc concentrations differed significantly between slopes (Welch's *t*-test, $p < 0.05$; Figure 2b), with higher mean concentrations on the southern slope (184.66 ± 201.35 mg kg^{-1}, σ) than on the northern slope (66.70 ± 27.08 mg kg^{-1}, σ). Mean concentrations of Co, Ni, Pb, and As were also generally higher on the southern slope (13.64 ± 12.32 mg kg^{-1}, 21.58 ± 21.77 mg kg^{-1}, 21.91 ± 28.82 mg kg^{-1}, and 4.16 ± 2.89 mg kg^{-1}, respectively) than on the northern slope (7.01 ± 4.77 mg kg^{-1}, 10.87 ± 11.98 mg kg^{-1}, 11.67 ± 11.98 mg kg^{-1}, and 2.98 ± 1.77 mg kg^{-1}), although these differences were not statistically significant.

Overall, the southern slope was characterized by lighter Zn isotopic compositions accompanied by higher trace metal concentrations, whereas the northern slope exhibited heavier δ^{66}Zn values and lower metal concentrations.

3.2. Elevational Distributions of Zn Isotopes and Metal Concentrations

On the southern slope, Zn isotopic compositions showed a significant non-linear relationship with elevation ($p < 0.01$), with δ^{66}Zn values shifting from lighter to heavier values with increased elevation. The lightest δ^{66}Zn value (−0.41‰) occurred at 950 m, whereas higher elevations were associated with heavier δ^{66}Zn values. In contrast, Zn isotopic compositions on the northern slope were confined to a narrower and heavier range, with no significant relationship with elevation.

Concentrations of Zn, Pb, Ni, Co, and As on the southern slope were fitted using a Generalized Additive Models (GAMs) (details are available in Supporting Information S1), revealing significant relationships with elevation ($p < 0.01$), with R^2 values ranging from 0.49 to 0.75 (Figure 3). The fitted curves show higher concentrations at low elevations, decreasing toward mid-elevations, followed by a slight increase or a tendency toward stabilization at higher elevations. In contrast, trace metal concentrations on the northern slope showed an overall increasing trend with elevation (Figure 3).

Overall, the southern slope displayed an altitudinal pattern characterized by higher trace metal concentrations and lighter δ^{66}Zn values at low elevations (−0.41‰ to +0.07‰, <2,000 m), transitioning to lower metal

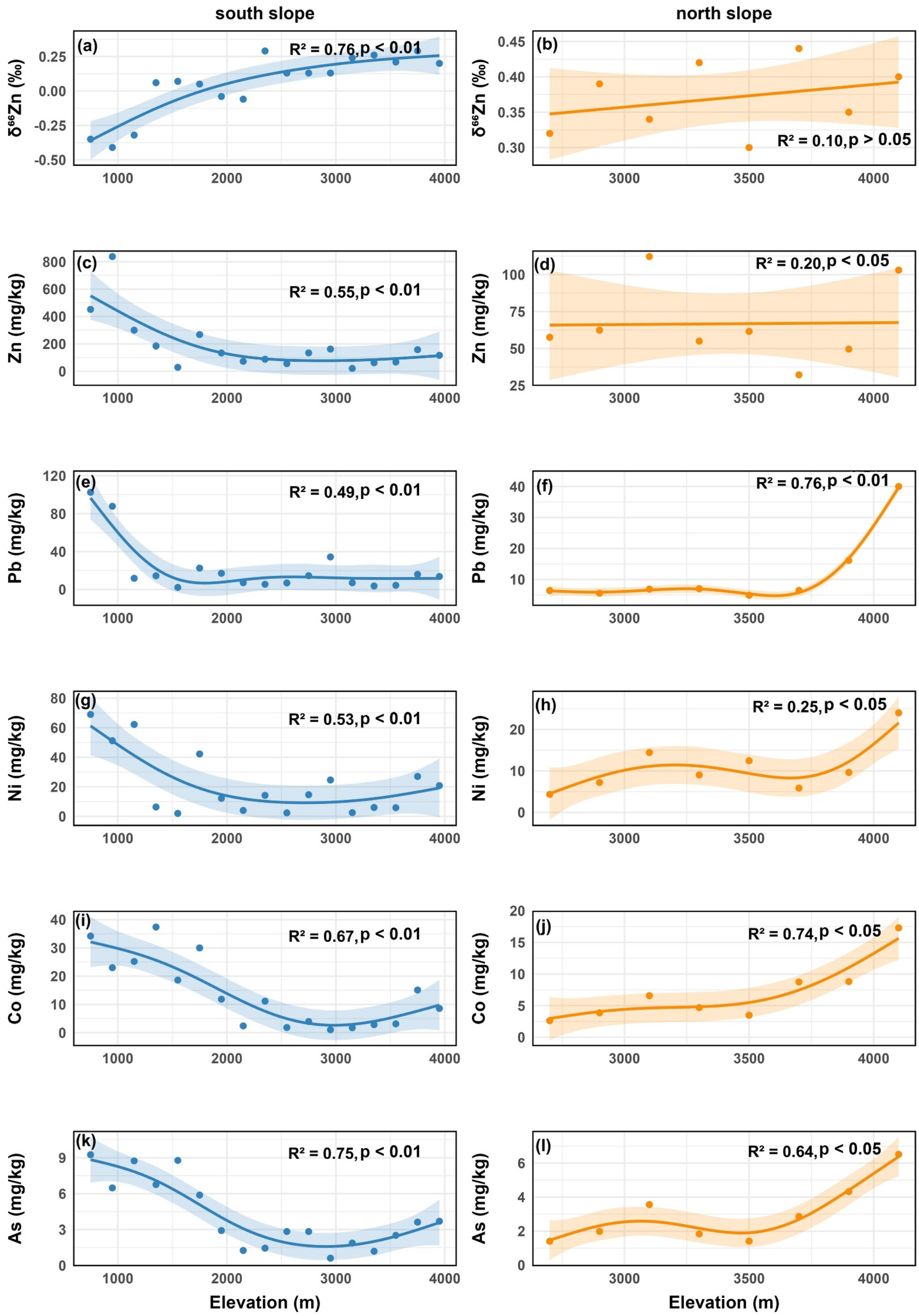

Figure 3. Altitudinal variation of δ^{66}Zn (a, b) and trace metal concentrations (Zn, Pb, Ni, Co, As) (c–l) measured in moss samples along the south (left column) and north (right column) slopes. Points are sample values; solid lines are Generalized Additive Models fits with 95% confidence intervals (shaded).

concentrations and heavier δ^{66}Zn values at higher elevations (+0.30‰ to +0.44‰, >3,000 m). By contrast, the northern slope was characterized by lower metal concentrations, increasing concentrations toward higher elevations, and consistently heavier Zn isotopic compositions with weak altitudinal variability.

4. Discussion

4.1. Atmospheric Deposition of Trace Metals Along Himalayan Slopes

Metal concentrations in mosses served as proxies for spatial variations in atmospheric deposition. The annual atmospheric input accumulation estimated from Monte Carlo simulations shows clear differences between the southern and northern slopes of the Himalayas, with higher atmospheric input fluxes of Zn, Pb, Ni, Co, and As on the southern slope compared to the northern slope (Figure S1 in Supporting Information S1). Accumulated inputs of trace metals peaked at low elevations, where contamination factors and enrichment factors showed elevated contamination (Tables S2 and S3 in Supporting Information S1), likely reflecting influence from near surface anthropogenic sources (Anjum et al., 2025; Guttikunda & Jawahar, 2014; Migaszewski et al., 2009).

On the southern slope, the contamination factor (CF) and enrichment factor (EF) values of all elements are generally high, with persistently elevated levels at low elevations (EF > 10, CF > 8; Figure S2 in Supporting Information S1), indicating stronger contamination and enrichment in these areas. In contrast, CF and EF on the northern slope exhibit an overall increasing trend with elevation (GAM, $p < 0.05$), with higher levels observed at high elevations (Figure S2 in Supporting Information S1). These patterns are consistent with the elevational distribution of elemental concentrations, suggesting clear differences in pollution levels and their spatial distribution between the two slopes.

Overall, accumulated inputs of trace metals from the atmosphere were higher at low elevations (<2,000 m) on the southern slope, with elevated contamination levels and enrichment. On the northern slope, the highest accumulation and elevated contamination and enrichment occurred at high elevations (>3,500 m). These patterns highlight contrasting altitudinal distributions of trace metals across the two slopes of the Himalayas.

4.2. Controlling Factors of the Altitudinal Distribution Patterns of Trace Metals

4.2.1. Anthropogenic Activities

As the summer monsoon windward side of the Himalayas, the southern slope directly receives atmospheric pollutants from high-intensity source regions in South Asia, including industrial activities, traffic emissions, and coal combustion. Elevated concentrations at low elevations (As: 9.26 mg kg^{-1}; Pb: 102.60 mg kg^{-1}; Zn: 452.00 mg kg^{-1}; Ni: 69.00 mg kg^{-1}; Co: 37.40 mg kg^{-1}) far exceed values reported for remote background regions. Moss surveys in Alaska, a minimally impacted region, reported much lower levels (Zn: 44.70 mg kg^{-1}; Ni: 4.70 mg kg^{-1}; Co: 1.40 mg kg^{-1}; As: ≤1.00 mg kg^{-1}) (Migaszewski et al., 2009). Relative to these baselines, Zn, Ni, and Co are elevated by about one order of magnitude, with As approaching a similar enhancement.

Such enrichment is unlikely to reflect natural variability and instead indicates substantial anthropogenic inputs. This is consistent with aerosol vertical profiles in Himalayan valleys, which show high pollutant loadings near the southern foothills and decreasing concentrations with elevation (Babu et al., 2011; Yuan et al., 2020). For example, aerosol observations in Nepal show Zn concentrations of 497–2,193 ng m^{-3}, with enrichment factors (EF_{Zn}) reaching up to 201.5, while Ni, Co, and Pb also exhibit elevated concentrations and enrichment characteristics indicative of strong anthropogenic sources. Similarly, the Indo-Gangetic Plain shows high levels of trace metal pollution and associated environmental risks, reflecting intensive industrial and vehicular emissions (Kang et al., 2019; Rawat et al., 2021, 2024).

Differences in source characteristics further control transport. Metal smelting mainly releases pollutants into the near-surface atmosphere, causing strong low-elevation contamination, whereas fine particles from coal combustion and biomass burning are efficiently transported over long distances and can reach high altitudes (D. Li et al., 2024; Sivry et al., 2008). The increase in δ^{66}Zn from negative to positive values with elevation provides geochemical evidence for this shift, indicating a transition from isotopically light Zn derived from near-surface smelting to heavier Zn associated with high-altitude aerosols influenced by coal combustion.

In contrast, anthropogenic activity on the northern slope is limited, with emissions mainly from residential coal use and transportation and no large-scale industry or smelting. These local sources alone cannot explain the observed high-elevation enrichment (Zn: 103.00 mg kg^{-1}; Co: 17.30 mg kg^{-1}; Ni: 24.00 mg kg^{-1}; Pb: 40.00 mg kg^{-1}; As: 6.52 mg kg^{-1}). A more plausible explanation is transboundary transport of fine particulate heavy metals from South Asia, particularly the Indo-Gangetic Plain and Nepal.

4.2.2. Meteorological and Topographic Controls

Once anthropogenic metals enter mountain environments, their spatial patterns are controlled by meteorology and topography, which regulate deposition processes. Elevation gradients modify temperature and precipitation, influencing dry and wet deposition and producing marked altitudinal differences in trace metal accumulation (H. Zhang et al., 2013).

On the southern slope, the windward side of the Himalayas, the Indian summer monsoon brings abundant precipitation (>2,000 mm yr^{-1} in Motuo). Pollutants are transported along deeply incised valleys by monsoonal circulation and upper-level westerlies, and efficient wet scavenging concentrates atmospheric inputs at low elevations, resulting in higher moss-recorded metal accumulation (Figure S1 in Supporting Information S1) (Bing et al., 2018; Liu et al., 2023). With increasing elevation, condensation-related processes become more important, and cloud and fog deposition enhances fine aerosol removal, leading to a slight increase in metal accumulation above 3,000 m (Figure 3). Similar altitudinal patterns have been reported in other high-altitude regions based on multiple environmental archives, including moss biomonitoring, soils, and precipitation (Bing et al., 2018; T. Li et al., 2017; Xiao et al., 2021).

The northern slope is affected by a strong rain shadow, where limited precipitation reduces wet deposition and increases the relative importance of dry deposition (Cherednichenko et al., 2021). Under the combined influence of regional topography and monsoon circulation, aerosols from South Asia are advected into the interior of the Tibetan Plateau (R. Zhang et al., 2015; M. Zhang et al., 2020; Y. Zhang et al., 2020). Topographically induced airflow convergence and mountain trapping further favor pollutant retention and accumulation at high elevations.

4.2.3. Vegetation Effects

Spatial variations in vegetation cover also influence the transport and deposition of atmospheric trace metals. The Yarlung Tsangpo Grand Canyon region exhibits dense vegetation, with NDVI > 0.6 below 3,000 m and well-developed forests (H. Li et al., 2016; Yu et al., 2022). On the southern slope, forest canopies intercept pollutants through stomatal uptake and foliar adsorption. During rainfall, retained metals are washed off, producing metal-enriched throughfall (He et al., 2023; Tan et al., 2019) that enhances trace metal inputs to understory mosses.

Observations from Mount Gongga show that trace metal concentrations in throughfall exceed those in open precipitation and decrease with elevation (Bing et al., 2018). Mosses therefore accumulate metals from enriched throughfall and surface runoff, leading to increased concentrations and altered spatial patterns (Gandois et al., 2010; T. Li et al., 2017). In contrast, vegetation on the northern slope is sparse, especially at high elevations where alpine meadows and shrublands dominate. Under these conditions, mosses act as primary receptors of atmospheric deposition, directly capturing airborne particles. Consequently, trace metal accumulation is less affected by vegetation filtering and more directly reflects atmospheric inputs.

To evaluate the effects of environmental factors on the spatial distribution of Zn isotopes (δ^{66}Zn), a multiple linear regression model was applied to quantify their relative contributions to δ^{66}Zn variability (Text S3 in Supporting Information S1). The factor contributions of elevation, anthropogenic activity, and vegetation coverage to δ^{66}Zn spatial variability in the region are 44.2%, 28.8%, and 26.9%, respectively ($R^2 = 0.82$, $p < 0.01$). The interaction among factors is negligible ($\Delta R^2 = 0.006$), indicating limited synergistic effects. Overall, elevation-associated environmental conditions play a dominant role in controlling the spatial distribution of δ^{66}Zn and metal concentrations.

4.3. Source Apportionment of Heavy Metal Pollutants Constrained by Zinc Isotopes

Stable zinc isotopes (δ^{66}Zn) were used as a tracer for source discrimination, assuming conservative behavior during atmospheric transport and moss uptake, as isotopic fractionation in mosses is negligible (Cloquet et al., 2008). Accordingly, δ^{66}Zn values were taken to represent atmospheric inputs. A Bayesian mixing model (MixSIAR) was applied (Table S4 in Supporting Information S1) to quantify the relative contributions of four major sources—coal combustion, metal smelting, natural dust, and non-exhaust traffic emissions—and their altitudinal variations on the southern and northern slopes.

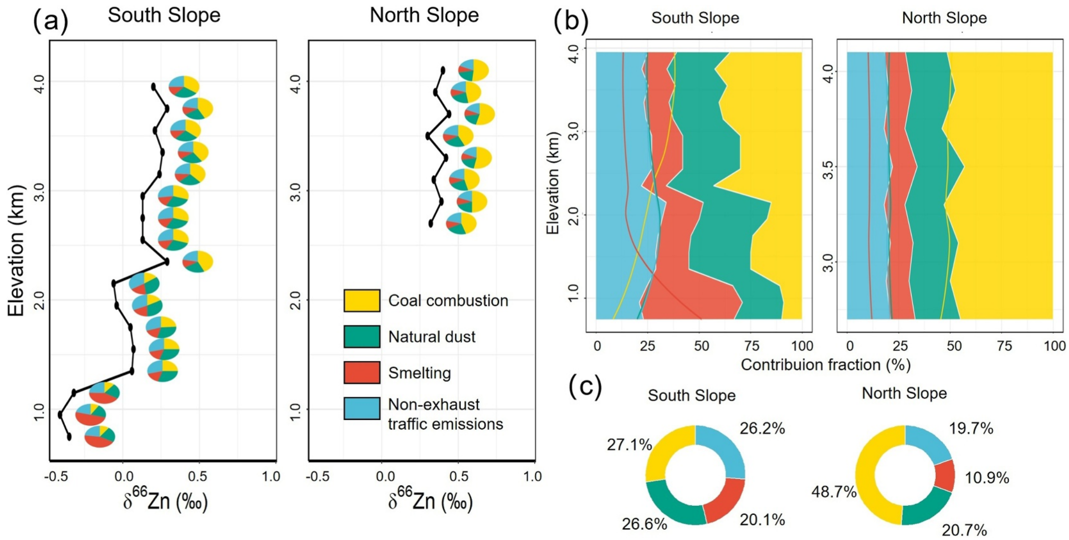

Figure 4. Zn source apportionment in mosses from the southern and northern slopes based on δ^{66}Zn of potential sources, including natural dust (+0.25 ± 0.15‰), smelting (−0.68 ± 0.07‰), coal combustion (+1.31 ± 0.11‰), and non-exhaust traffic emissions (+0.22 ± 0.07‰). (a) Altitudinal variations in δ^{66}Zn and Bayesian-estimated source contributions; (b) Stacked bars showing elevation-dependent contributions of sources, with LOESS-smoothed trends; (c) Slope-averaged contributions of each source.

On the southern slope, source contributions show clear altitudinal differentiation. At low elevations (<1,150 m), smelting dominates (42%–50%), consistent with the region acting as a near-source receptor of South Asian industrial emissions. Smelting releases isotopically light Zn, producing lower δ^{66}Zn values (Mattielli et al., 2009; Sivry et al., 2008). With increasing elevation, smelting contributions decline to 12%–18%, while coal combustion increases markedly from ∼10% to up to 42% (Figure 4a). This shift indicates increasing influence of coal-derived fine aerosols (e.g., fly ash and soot) transported at higher altitudes and characterized by heavier isotopic signatures (Toutain et al., 2008; Wu et al., 2024). In contrast, natural dust and non-exhaust traffic emissions vary little with elevation, averaging 26.6% and 26.2%, respectively (Figure 4c).

The northern slope exhibits a vertically uniform mixed-source pattern. Coal combustion consistently represents the largest contribution (43%–54%) across all elevations, consistent with long-range transport influencing the interior of the Tibetan Plateau (Wei et al., 2025; Wu et al., 2024). Smelting contributions remain low (10%–12%) and show minimal altitudinal change (Figure 4b), indicating limited local industrial influence and restricted cross-barrier transport of direct industrial emissions. Natural dust and non-exhaust traffic emissions also show weak variability, with mean contributions of 20.7% and 19.7%, respectively (Figure 4c). Mosses integrate atmospheric deposition over months to years and record ambient Zn levels over their growth period, which in our study region mainly occurs from June to September, coinciding with the Indian summer monsoon. Backward trajectory and wind field analyses (Figure 1 and Figure S3 in Supporting Information S1) indicate that air masses during the sampling period were predominantly controlled by the Indian summer monsoon, facilitating the transport of pollutants from South Asia to the Tibetan Plateau. Given the relatively stable isotopic signatures of dominant sources, moss δ^{66}Zn primarily records monsoon-driven transboundary transport.

4.4. Transboundary Transport and Cross-Himalayan Deposition Mechanisms of Pollutants

Integrating source apportionment with trace metal distributions reveals distinct pollution regimes and transport pathways across the Himalayas. On the southern slope, the Yarlung Tsangpo Grand Canyon acts as a major corridor for transboundary pollutants from South Asia, with deposition controlled by strong source inputs and elevation-dependent scavenging. At low elevations (<2,000 m), efficient wet deposition concentrates particulate pollutants, accompanied by high contributions of isotopically light Zn from smelting, indicating dominant influence of near-surface anthropogenic emissions.

With increasing elevation, coarse particles are progressively removed, and fine aerosols from coal combustion become more important. These particles, characterized by relatively heavy δ^{66}Zn, are efficiently scavenged by cloud and fog, resulting in modest increases in metal inputs above 3,000 m, coal contributions of ∼35%–43%, and persistently positive isotopic values (Figure 4b). This vertical pattern reflects a shift from low-elevation deposition dominated by coarse smelting emissions to high-elevation inputs increasingly influenced by long-range transported coal-derived fine particles.

In contrast, the northern slope is mainly affected by cross-barrier transport of high-altitude aerosols enriched in heavy Zn isotopes. Upper-level circulation advects polluted air masses across the Himalayas (Figure S3 in Supporting Information S1), leading to consistently high coal combustion contributions (43%–54%) and enhanced metal accumulation above 3,500 m. These patterns indicate that long-range atmospheric transport and high-elevation deposition, rather than local emissions, dominate trace metal inputs on the northern slope and the interior of the Tibetan Plateau.

5. Conclusion

This study applies moss Zn isotopic compositions to constrain the sources and cross-border transport of anthropogenic heavy metals (Zn, Pb, As, Ni, Co) across the Himalayas. Pronounced altitudinal gradients in metal concentrations and δ^{66}Zn (−0.41‰ to 0.29‰) on the southern slope indicate a transition from local industrial emissions (42%–50%) at low elevations to increasing contributions from long-range transported coal combustion at higher elevations. On the northern slope, lower metal loads but systematically heavier δ^{66}Zn values (0.30‰ to 0.44‰) suggest a dominant influence of transported coal-derived emissions (43%–54%). Topography, anthropogenic activities, and vegetation coverage collectively regulate the vertical distribution of pollutants. These results provide isotopic evidence that anthropogenic emissions from South Asia, particularly coal combustion, can cross the Himalayan barrier and influence the atmospheric environment of the southern Tibetan Plateau. However, the limited availability of atmospheric Zn isotopic data in remote regions constrains direct comparison. Future work incorporating in situ aerosol Zn isotope observations, particularly at high elevations, is needed to further resolve transboundary transport processes.

Conflict of Interest

The authors declare no conflicts of interest relevant to this study.

Availability Statement

Analysis of atmospheric mass track from the https://www.ready.noaa.gov/hypub-bin/trajasrc.pl. The data used in this paper have been made available through the tables and Supporting Information uploaded to the submission. Moreover, the all data presented in this article are available through the Figshare data repository at https://doi.org/10.6084/m9.figshare.31354543 (Jiao, 2026). The data will eventually be deposited in the Figshare data repository by the time the article is accepted, and that the data is available in the supporting information, tables, and/or figures during peer review.

Acknowledgments

This work was supported by the National Natural Science Foundation of China (42371139), National Key R&D Program of China (2024YFF1308105); the Fundamental Research Funds for the Central Universities, the China University of Geosciences (Wuhan) (No. CUG260602); And by the "CUG Scholar" Scientific Research Funds at China University of Geosciences (Wuhan) (Project No. 2023092), by the Gansu Province Natural Science Foundation Key Project (23JRRA858). The authors would like also to thank the work team for their hard work in the fieldwork observation of the Tibetan Plateau and Himalayas during 2024.

References

Anjum, M., Siddique, N., Younis, H., Shafique, M. A., Munawar, S., Zubair, M., et al. (2025). Chemometric assessment, seasonal variation and source apportionment of air pollutants in Islamabad's industrial area. *Journal of Trace Elements and Minerals*, *12*, 100244. https://doi.org/10.1016/j.jtemin.2025.100244

Babu, S. S., Chaubey, J. P., Krishna Moorthy, K., Gogoi, M. M., Kompalli, S. K., Sreekanth, V., et al. (2011). High altitude (∼4520 m asl) measurements of black carbon aerosols over western trans-Himalayas: Seasonal heterogeneity and source apportionment. *Journal of Geophysical Research*, *116*(D24), D24201. https://doi.org/10.1029/2011JD016722

Bing, H., Wu, Y., Li, J., Xiang, Z., Luo, X., Zhou, J., et al. (2019). Biomonitoring trace element contamination impacted by atmospheric deposition in China's remote mountains. *Atmospheric Research*, *224*, 30–41. https://doi.org/10.1016/j.atmosres.2019.03.018

Bing, H., Zhou, J., Wu, Y., Luo, X., Xiang, Z., Sun, H., et al. (2018). Barrier effects of remote high mountain on atmospheric metal transport in the eastern Tibetan Plateau. *Science of The Total Environment*, *628–629*, 687–696. https://doi.org/10.1016/j.scitotenv.2018.02.035

Borrok, D. M., Gieré, R., Ren, M., & Landa, E. R. (2010). Zinc isotopic composition of particulate matter generated during the combustion of coal and coal + tire-derived fuels. *Environmental Science & Technology*, *44*(23), 9219–9224. https://doi.org/10.1021/es102439g

Bunnell, Z. B., Sieber, M., Hamilton, D. S., Marsay, C. M., Buck, C. S., Landing, W. M., et al. (2025). The influence of natural, anthropogenic, and wildfire sources on iron and zinc aerosols delivered to the North Pacific Ocean. *Geophysical Research Letters*, *52*(3), e2024GL113877. https://doi.org/10.1029/2024GL113877

Cai, X., Yuan, W., Zhang, Q., Luo, K., Xu, Y., Zhang, G., et al. (2024). Quantifying altitudinal Mercury accumulation in biomonitors along Himalayan Valleys using Mercury isotopes. *Environmental Science & Technology*, *58*(50), 22183–22193. https://doi.org/10.1021/acs.est.4c10224

Cherednichenko, V. S., Cherednichenko, A. V., Cherednichenko, A. V., Zheksenbaeva, A. K., & Madibekov, A. S. (2021). Heavy metal deposition through precipitation in Kazakhstan. *Heliyon*, *7*(1), e05844. https://doi.org/10.1016/j.heliyon.2020.e05844

Cloquet, C., Carignan, J., Lehmann, M. F., & Vanhaecke, F. (2008). Variation in the isotopic composition of zinc in the natural environment and the use of zinc isotopes in biogeosciences: A review. *Analytical and Bioanalytical Chemistry*, *390*(2), 451–463. https://doi.org/10.1007/s00216-007-1635-y

Dhungel, S., Kathayat, B., Mahata, K., & Panday, A. (2018). Transport of regional pollutants through a remote Trans-Himalayan valley in Nepal. *Atmospheric Chemistry and Physics*, *18*(2), 1203–1216. https://doi.org/10.5194/acp-18-1203-2018

Dolgopolova, A., Weiss, D. J., Seltmann, R., Kober, B., Mason, T. F. D., Coles, B., & Stanley, C. J. (2006). Use of isotope ratios to assess sources of Pb and Zn dispersed in the environment during mining and ore processing within the Orlovka–Spokoinoe mining site (Russia). *Applied Geochemistry*, *21*(4), 563–579. https://doi.org/10.1016/j.apgeochem.2005.12.014

Dong, S., Weiss, D. J., Strekopytov, S., Kreissig, K., Sun, Y., Baker, A. R., & Formenti, P. (2013). Stable isotope ratio measurements of Cu and Zn in mineral dust (bulk and size fractions) from the Taklimakan Desert and the Sahel and in aerosols from the eastern tropical North Atlantic Ocean. *Talanta*, *114*, 103–109. https://doi.org/10.1016/j.talanta.2013.03.062

Dong, Z., Brahney, J., Kang, S., Elser, J., Wei, T., Jiao, X., & Shao, Y. (2020). Aeolian dust transport, cycle and influences in high-elevation cryosphere of the Tibetan Plateau region: New evidences from alpine snow and ice. *Earth-Science Reviews*, *211*, 103408. https://doi.org/10.1016/j.earscirev.2020.103408

Duan, Y., Wang, Z., Gou, W., Wang, Z., Li, Q., & Li, W. (2025). Stable zinc isotopes as tracers in environmental geochemistry. *Earth-Science Reviews*, *269*, 105185. https://doi.org/10.1016/j.earscirev.2025.105185

Elsen, P. R., Monahan, W. B., & Merenlender, A. M. (2020). Topography and human pressure in mountain ranges alter expected species responses to climate change. *Nature Communications*, *11*(1), 1974. https://doi.org/10.1038/s41467-020-15881-x

Gandois, L., Tipping, E., Dumat, C., & Probst, A. (2010). Canopy influence on trace metal atmospheric inputs on forest ecosystems: Speciation in throughfall. *Atmospheric Environment*, *44*(6), 824–833. https://doi.org/10.1016/j.atmosenv.2009.11.028

Gelly, R., Fekiacova, Z., Guihou, A., Doelsch, E., Deschamps, P., & Keller, C. (2019). Lead, zinc, and copper redistributions in soils along a deposition gradient from emissions of a Pb-Ag smelter decommissioned 100 years ago. *Science of The Total Environment*, *665*, 502–512. https://doi.org/10.1016/j.scitotenv.2019.02.092

Guttikunda, S. K., & Jawahar, P. (2014). Atmospheric emissions and pollution from the coal-fired thermal power plants in India. *Atmospheric Environment*, *92*, 449–460. https://doi.org/10.1016/j.atmosenv.2014.04.057

He, L., Wang, S., Liu, M., Chen, Z., Xu, J., & Dong, Y. (2023). Transport and transformation of atmospheric metals in ecosystems: A review. *Journal of Hazardous Materials Advances*, *9*, 100218. https://doi.org/10.1016/j.hazadv.2022.100218

Hong, S., Lee, K., Hou, S., Hur, S. D., Ren, J., Burn, L. J., et al. (2009). An 800-Year record of atmospheric As, Mo, Sn, and Sb in central Asia in high-altitude ice cores from Mt. Qomolangma (Everest), himalayas. *Environmental Science & Technology*, *43*(21), 8060–8065. https://doi.org/10.1021/es901685u

Jeong, H., Ryu, J. S., & Ra, K. (2022). Characteristics of potentially toxic elements and multi-isotope signatures (Cu, Zn, Pb) in non-exhaust traffic emission sources. *Environmental Pollution*, *292*, 118339. https://doi.org/10.1016/j.envpol.2021.118339

Jiao, X. (2026). Data of Zinc isotopes reveal cross-border transport of coal combustion pollutants across the Himalayas during the summer monsoon [Dataset]. *figshare*. https://doi.org/10.6084/m9.figshare.31354543

Kang, S., Zhang, Q., Qian, Y., Ji, Z., Li, C., Cong, Z., et al. (2019). Linking atmospheric pollution to cryospheric change in the third pole Region: Current progresses and future prospects. *National Science Review*, *6*(4), 796–809. https://doi.org/10.1093/nsr/nwz031

Kim, D. M., Batsaikhan, B., Yun, S. T., Im, D. G., & Seo, H. S. (2025). Comprehensive multimetal isotopic model for regional-scale water management in a mining city: Tracing contamination sources, pathways, and geochemical processes using Cu, Mo, S-O, and Zn isotopes. *Journal of Hazardous Materials*, *494*, 138562. https://doi.org/10.1016/j.jhazmat.2025.138562

Li, D., Liu, H., Liu, J., Li, J., & Wang, K. (2024). Impacts of anthropogenic emissions and open biomass burning in south Asia and Southeast Asia on air quality and meteorology over Southern China. *Journal of Geophysical Research: Atmospheres*, *129*(17), e2024JD041267. https://doi.org/10.1029/2024JD041267

Li, H., Jiang, J., Chen, B., Li, Y., Xu, Y., & Shen, W. (2016). Pattern of NDVI-based vegetation greening along an altitudinal gradient in the eastern Himalayas and its response to global warming. *Environmental Monitoring and Assessment*, *188*(3), 186. https://doi.org/10.1007/s10661-016-5196-4

Li, T., Wang, Y., Zhou, J., Wang, T., Ding, A., Nie, W., et al. (2017). Evolution of trace elements in the planetary boundary layer in southern China: Effects of dust storms and aerosol-cloud interactions. *Journal of Geophysical Research: Atmospheres*, *122*(6), 3492–3506. https://doi.org/10.1002/2016JD025541

Liu, W., Zhao, C., Xu, M., Feng, J., Du, Q., Gu, J., et al. (2023). Southern Himalayas rainfall as a key driver of interannual variation of pre-monsoon aerosols over the Tibetan Plateau. *npj Climate and Atmospheric Science*, *6*(1), 57. https://doi.org/10.1038/s41612-023-00392-5

Mattielli, N., Petit, J. C. J., Deboudt, K., Flament, P., Perdrix, E., Taillez, A., et al. (2009). Zn isotope study of atmospheric emissions and dry depositions within a 5 km radius of a Pb–Zn refinery. *Atmospheric Environment*, *43*(6), 1265–1272. https://doi.org/10.1016/j.atmosenv.2008.11.030

Migaszewski, Z. M., Gałuszka, A., Crock, J. G., Lamothe, P. J., & Dołęgowska, S. (2009). Interspecies and interregional comparisons of the chemistry of PAHs and trace elements in mosses Hylocomium splendens (Hedw.) B.S.G. and Pleurozium schreberi (Brid.) Mitt. from Poland and Alaska. *Atmospheric Environment*, *43*(7), 1464–1473. https://doi.org/10.1016/j.atmosenv.2008.11.035

Musah, B. I., Yang, J., & Xu, G. (2025). Drivers of toxic element accumulation in terrestrial ecosystems across elevational gradients. *Ecological Indicators*, *174*, 113446. https://doi.org/10.1016/j.ecolind.2025.113446

Nizam, S., Sen, I. S., Vinoj, V., Galy, V., Selby, D., Azam, M. F., et al. (2020). Biomass-Derived provenance dominates glacial Surface organic carbon in the Western himalaya. *Environmental Science & Technology*, *54*(14), 8612–8621. https://doi.org/10.1021/acs.est.0c02710

Ochoa Gonzalez, R., & Weiss, D. (2015). Zinc isotope variability in three coal-fired power plants: A predictive model for determining isotopic fractionation during combustion. *Environmental Science & Technology*, *49*(20), 12560–12567. https://doi.org/10.1021/acs.est.5b02402

Rawat, B., Shrma, C. M., Tripathee, L., Wan, X., Cong, Z., Paudyal, R., et al. (2024). Concentration, seasonality, and sources of trace elements in atmospheric aerosols from Godavari in the southern Himalayas. *Environment and Pollution*, *344*, 123359.

Rawat, B., Zhang, Q. G., Shrma, C. M., Tripathee, L., Pandey, A., Kandel, K., et al. (2021). Glacial record of trace metal pollution over the Central Himalayas and its surroundings: Distribution, variation, and anthropogenic signals. *Atmospheric Research*, *251*, 105428. https://doi.org/10.1016/j.atmosres.2020.105428

Reddington, C. L., Conibear, L., Knote, C., Silver, B. J., Li, Y. J., Chan, C. K., et al. (2019). Exploring the impacts of anthropogenic emission sectors on PM2.5 and human health in South and East Asia. *Atmospheric Chemistry and Physics*, *19*(18), 11887–11910. https://doi.org/10.5194/acp-19-11887-2019

Schleicher, N. J., Dong, S., Packman, H., Little, S. H., Ochoa Gonzalez, R., Najorka, J., et al. (2020). A global assessment of copper, zinc, and lead isotopes in mineral dust sources and aerosols. *Frontiers of Earth Science*, *8*, 167. https://doi.org/10.3389/feart.2020.00167

Schleicher, N. J., & Weiss, D. J. (2023). Identification of atmospheric particulate matter derived from coal and biomass burning and from non-exhaust traffic emissions using zinc isotope signatures. *Environmental Pollution*, *329*, 121664. https://doi.org/10.1016/j.envpol.2023.121664

Sen, I. S., & Peucker-Ehrenbrink, B. (2012). Anthropogenic disturbance of element cycles at the Earth's surface. *Environmental Science & Technology*, *46*(16), 8601–8609. https://doi.org/10.1021/es301261x

Sivry, Y., Riotte, J., Sonke, J. E., Audry, S., Schäfer, J., Viers, J., et al. (2008). Zn isotopes as tracers of anthropogenic pollution from Zn-ore smelters the Riou Mort–Lot River system. *Chemical Geology*, *255*(3–4), 295–304. https://doi.org/10.1016/j.chemgeo.2008.06.038

Tan, S., Zhao, H., Yang, W., Tan, B., Yue, K., Zhang, Y., et al. (2019). Forest Canopy can efficiently filter trace metals in deposited precipitation in a Subalpine spruce plantation. *Forests*, *10*(4), 318. https://doi.org/10.3390/f10040318

Tian, H. Z., Zhu, C. Y., Gao, J. J., Cheng, K., Hao, J. M., Wang, K., et al. (2015). Quantitative assessment of atmospheric emissions of toxic heavy metals from anthropogenic sources in China: Historical trend, spatial distribution, uncertainties, and control policies. *Atmospheric Chemistry and Physics*, *15*(17), 10127–10147. https://doi.org/10.5194/acp-15-10127-2015

Toutain, J.-P., Sonke, J., Munoz, M., Nonell, A., Polvé, M., Viers, J., et al. (2008). Evidence for Zn isotopic fractionation at Merapi volcano. *Chemical Geology*, *253*(1–2), 74–82. https://doi.org/10.1016/j.chemgeo.2008.04.007

Wei, T., Dong, Z., Li, F., Kang, S., & Qin, X. (2025). Quantifying the distribution and origins of aerosol zinc across the Northern Hemisphere using stable zinc isotopes: A review. *Journal of Hazardous Materials*, *491*, 137828. https://doi.org/10.1016/j.jhazmat.2025.137828

Wu, C. H., Hsu, H. H., & Chou, M. D. (2014). Effect of the Arakan Mountains in the northwestern Indochina Peninsula on the late May Asian monsoon transition: Arakan Mountains effect on Asian Monsoon. *Journal of Geophysical Research: Atmospheres*, *119*(18), 10769–10779. https://doi.org/10.1002/2014JD022024

Wu, R., Dong, Z., Yan, Y., Parteli, E., Wei, T., Li, F., et al. (2024). Zn isotope tracing unveils primary anthropogenic Zn sources in glacial cryoconite of the high Asian Mountains. *Journal of Geophysical Research: Atmospheres*, *129*(20), e2024JD041467. https://doi.org/10.1029/2024JD041467

Xiao, J., Han, X., Sun, S., Wang, L., & Rinklebe, J. (2021). Heavy metals in different moss species in alpine ecosystems of Mountain Gongga, China: Geochemical characteristics and controlling factors. *Environmental Pollution*, *272*, 115991. https://doi.org/10.1016/j.envpol.2020.115991

Xu, H., He, J., Li, J., Ren, H., Zhang, L., Gong, S., et al. (2023). Identifying spatio-temporal climatic characteristics and events of the South-Asian aerosol pollution transport to the Tibetan Plateau. *Atmospheric Research*, *286*, 106683. https://doi.org/10.1016/j.atmosres.2023.106683

Yan, H., Huang, J., He, Y., Liu, Y., Wang, T., & Li, J. (2020). Atmospheric water vapor budget and its long-term trend over the Tibetan Plateau. *Journal of Geophysical Research: Atmospheres*, *125*(23), e2020JD033297. https://doi.org/10.1029/2020JD033297

Yao, T., Thompson, L., Chen, D., & Piao, S. (2022). Reflections and future strategies for Third Pole Environment. *Nature Reviews Earth & Environment*, *3*(10), 608–610. https://doi.org/10.1038/s43017-022-00342-4

Yu, B., Yang, L., Liu, H., Xiao, C., Bu, D., Zhang, Q., et al. (2022). Tracing the transboundary transport of Mercury to the Tibetan Plateau using atmospheric Mercury isotopes. *Environmental Science & Technology*, *56*(3), 1568–1577. https://doi.org/10.1021/acs.est.1c05816

Yuan, Q., Wan, X., Cong, Z., Li, M., Liu, L., Shu, S., et al. (2020). In situ observations of light-absorbing carbonaceous aerosols at Himalaya: Analysis of the South Asian sources and trans-Himalayan Valleys transport pathways. *Journal of Geophysical Research: Atmospheres*, *125*(18), e2020JD032615. https://doi.org/10.1029/2020JD032615

Zhang, H., Yin, R., Feng, X., Sommar, J., Anderson, C. W. N., Sapkota, A., et al. (2013). Atmospheric mercury inputs in montane soils increase with elevation: Evidence from mercury isotope signatures. *Scientific Reports*, *3*(1), 3322. https://doi.org/10.1038/srep03322

Zhang, M., Zhao, C., Cong, Z., Du, Q., Xu, M., Chen, Y., et al. (2020). Impact of topography on black carbon transport to the southern Tibetan Plateau during the pre-monsoon season and its climatic implication. *Atmospheric Chemistry and Physics*, *20*(10), 5923–5943. https://doi.org/10.5194/acp-20-5923-2020

Zhang, R., Wang, H., Qian, Y., Rasch, P. J., Easter, R. C., Ma, P.-L., et al. (2015). Quantifying sources, transport, deposition, and radiative forcing of black carbon over the Himalayas and Tibetan Plateau. *Atmospheric Chemistry and Physics*, *15*(11), 6205–6223. https://doi.org/10.5194/acp-15-6205-2015

Zhang, Y., Wu, X., & Zheng, D. (2020). Vertical differentiation of land cover in the central Himalayas. *Journal of Geographical Sciences*, *30*(6), 969–987. https://doi.org/10.1007/s11442-020-1765-0

Zhu, C., Tian, H., & Hao, J. (2020). Global anthropogenic atmospheric emission inventory of twelve typical hazardous trace elements, 1995–2012. *Atmospheric Environment*, *220*, 117061. https://doi.org/10.1016/j.atmosenv.2019.117061

References From the Supporting Information

Stock, B. C., Jackson, A. L., Ward, E. J., Parnell, A. C., Phillips, D. L., & Semmens, B. X. (2018). Analyzing mixing systems using a new generation of Bayesian tracer mixing models. *PeerJ*, *6*, e5096. https://doi.org/10.7717/peerj.5096

Taylor, S. R., & McLennan, S. M. (1995). The geochemical evolution of the continental crust. *Reviews of Geophysics*, *33*(2), 241–265. https://doi.org/10.1029/95RG00262

Zechmeister, H. G., Hohenwallner, D., Riss, A., & Hanus-Illnar, A. (2003). Variations in heavy metal concentrations in the moss species Abietinella abietina (Hedw.) Fleisch. according to sampling time, within site variability and increase in biomass. *Science of The Total Environment*, *301*(1–3), 55–65. https://doi.org/10.1016/S0048-9697(02)00296-6